Calibrated Radio Interferometry and Galactic HI Kinematics

Hareethha Vellaichammy Suresh Babu

April 2025

Abstract

This practical employed a two-element radio interferometer at Bayfordbury Observatory, comprising the West and Mid dishes, to carry out high-resolution observations at the 1.4 GHz neutral hydrogen line. The principal aim was to extract fringe amplitudes from Cygnus A as a reference calibrator. A flux conversion factor was derived and subsequently applied to estimate the 1.4 GHz flux density of Cas A. The raw voltage signals were pre-processed through detrending and smoothing algorithms in Python to suppress instrumental drift and random noise, enabling accurate peak-to-peak amplitude extraction and robust signal characterization. Concurrently, a spectral survey of Galactic neutral hydrogen was conducted in single-dish mode. Sixty spectra were acquired across a wide span of Galactic longitudes and synthesized into a velocity–longitude map, revealing coherent kinematic structures and signatures of spiral arm morphology. While observational constraints—including bandwidth smearing and the absence of barycentric correction—introduced systematic limitations, the resulting flux estimates and emission patterns exhibited strong agreement with theoretical expectations and existing survey data, underscoring the reliability of both the methodology and instrumentation.

Contents

1 Introduction

Radio astronomy enables the investigation of astrophysical phenomena through their radio frequency emissions, offering access to structures and processes that are often obscured in the optical regime by interstellar dust. This practical comprised two core observational components: an interferometric study involving Cygnus A and Cassiopeia A to calibrate and measure radio flux densities, and a single-dish survey of neutral hydrogen to map the velocity structure of the Milky Way via its 21 cm spectral line.

Cygnus A is a powerful extragalactic radio source powered by an active galactic nucleus, where synchrotron emission from relativistic jets interacting with magnetic fields produces a strong, compact, and stable radio signal. Cassiopeia A, by contrast, is a Galactic supernova remnant whose radio emission arises from non-thermal synchrotron processes as relativistic electrons spiral through magnetic fields in the post-explosion environment.

The Milky Way's large-scale structure is traced through the 21 cm hyperfine transition of neutral hydrogen, which emits a narrow spectral line that shifts under the Doppler effect, allowing us to measure gas velocities along the line of sight. The Sun emits broadband radio radiation primarily from thermal bremsstrahlung and gyroresonance processes in its corona and active regions, often studied via continuum observations at longer wavelengths.

The section that follows details the experimental setup, data acquisition methods, signal processing techniques, and subsequent analysis for both the interferometric calibration and Galactic HI Survey, concluding with a comparison to established literature and a discussion of observational limitations.

2 Radio Interferometry: Cygnus A and Cas A

2.1 Instrument Setup and Configuration

To establish a clear understanding of the interferometric configuration, this section is structured into three parts: a description of the physical hardware and signal pathway, an explanation of the operating principle underlying fringe formation, and an analysis of the system's inherent observational limitations.

The interferometric observations were carried out using the West and Mid dishes of the Bayfordbury Observatory radio array. Each dish has a parabolic reflector of 3 m diameter and is equipped with a 21 cm receiver operating at a central frequency of 1.420 GHz, corresponding to the hyperfine transition of neutral hydrogen. The two-element configuration formed a single baseline of approximately 115 m, enabling spatial resolution sufficient to resolve compact astronomical radio sources. Incoming radio waves were converted into analog voltage signals by the receivers, which were subsequently digitized and recorded for further processing.

As the Earth rotates, the geometric path length between the two dishes changes with time for any fixed celestial source. This varying delay leads to a time-dependent phase difference between the received signals, which produces sinusoidal interference fringes in the correlated voltage output. The fringe frequency depends on the source's declination, the baseline orientation, and the time of observation. For sources near transit,

the projected baseline is maximal and the fringe contrast is strongest, enabling accurate amplitude measurements essential for flux calibration.

Despite its effectiveness for compact calibrator sources, the interferometric setup has several inherent limitations. One significant effect is *bandwidth smearing*, which arises from integrating over a finite frequency range. When the delay between antennas varies across the bandwidth, destructive interference reduces fringe visibility, particularly at long baselines and away from the transit. Additionally, the system's angular resolution is constrained by the fixed baseline length, making it less sensitive to extended or resolved sources such as Cassiopeia A. Finally, the absence of real-time delay compensation limits fringe quality when sources are not optimally positioned, introducing amplitude suppression and phase distortion into the recorded signals.

Figure 1: Mid and West radio dishes at Bayfordbury Observatory

2.1.1 Observing Parameters

Table 1: Instrument Configuration Parameters

Parameter	**Value**	**Purpose/Notes**
Start Channel	300	Defines lower limit of frequency scan range
End Channel	650	Sets upper limit of frequency scan range
Channels per step	5	Determines frequency resolution per integration
Offset	550	Sets central channel (used for tuning signal)
Gain	x50	Amplifies received voltage signal
Integration Time	0.3s	Time over which each data point is averaged
Repeats	1	Number of acquisitions per pointing (single sweep)

These parameters were selected to optimize signal clarity while maintaining manageable data volume. The integration time of 0.3 seconds strikes a balance between temporal resolution and noise suppression, while the use of 5 channels per step provides adequate spectral granularity across the 1.4GHz band. The gain factor ensures measurable fringe amplitudes from strong sources like Cygnus A, without saturating the receiver. By centering the scan around an offset of 550, the setup ensures symmetric coverage of the target frequency range while mitigating edge-channel artefacts.

2.2 Fringe Analysis and Calibration with Cygnus A

Cygnus A is a well-established calibrator in radio interferometry due to its high flux density, compact structure, and relatively stable emission. At a frequency of 1.4 GHz, it has a known flux density of 1579.96 Jy [1]. In this study, Cygnus A is used as a reference source to determine the interferometric system's gain and derive a calibration factor in Jy/V, enabling flux estimations of other observed sources.

2.2.1 Data Conditioning and Fringe Extraction

Raw voltage time series obtained from the interferometric system during Cygnus A observations were imported in CSV format. The signals, measured in millivolts over time, were initially pre-processed to remove non-numerical entries and suppress instrumental background. A linear detrending operation was applied to isolate the oscillatory component associated with fringe formation, followed by a five-point moving average filter to reduce high-frequency noise. This yielded a clean sinusoidal fringe signal corresponding to the changing geometric delay between antennas as the Earth rotated.

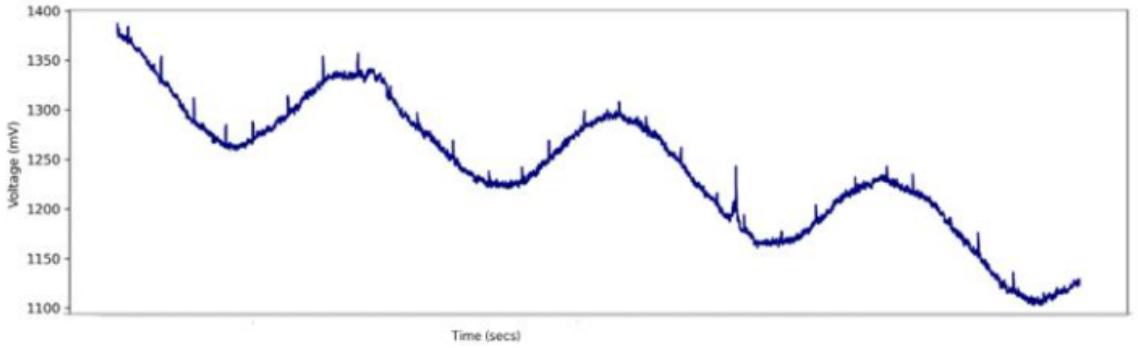

Figure 2: Interferometric Fringe Pattern from Cygnus A with Background Continuum trend

2.2.2 Amplitude Estimation

To estimate the voltage amplitude of the oscillating component, the peak-to-peak method was employed. The amplitude A was calculated as:

$$A = \frac{V_{\max} - V_{\min}}{2} \tag{1}$$

For Cygnus A, the measured peak-to-peak voltage was 53.00 mV, corresponding to an amplitude of:

$$A = \frac{53.00 \text{ mV}}{2} = 26.50 \text{ mV}$$

However, for calibration purposes, the full peak-to-peak voltage of 0.0530 V was used, consistent with the method employed in previous studies.

2.2.3 Calibration Factor Determination

The Jy/V calibration factor quantifies the relationship between measured fringe voltage and the source's known flux density. It was calculated as:

$$\text{Calibration Factor} = \frac{\text{Known Flux of Cygnus A (Jy)}}{\text{Measured Fringe Amplitude (V)}} \tag{2}$$

Given the known values:

- Cygnus A flux at 1.4 GHz = 1579.96 Jy [1]
- Measured fringe amplitude = 0.0530 V

The resulting calibration factor is:

$$\text{Calibration Factor} = \frac{1579.96}{0.0530} \approx 29{,}811.51 \text{ Jy/V}$$

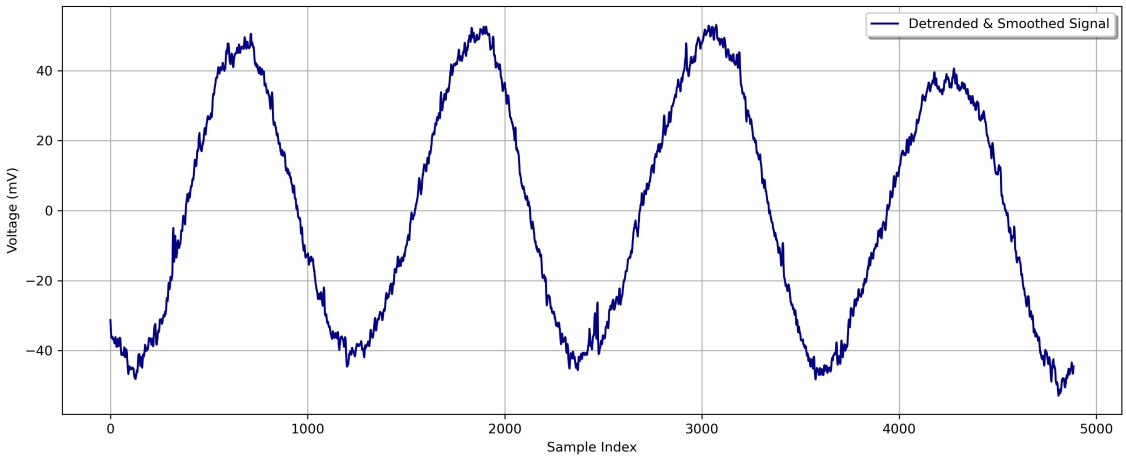

Figure 3: Detrended and Smoothed Cygnus A Fringe Signal Used for Flux Density Calibration

This calibration factor serves as a benchmark for converting voltage amplitudes of other astronomical sources into absolute flux density, assuming similar observing conditions and instrumental responses.

2.2.4 Discussion of Limitations

Although the calibration factor was derived under controlled and idealized conditions, real-world observations are subject to several uncertainties. These include signal decorrelation due to bandwidth smearing, finite baseline effects, thermal noise, and phase errors arising from environmental and instrumental instabilities. Such factors can lead to reduced fringe contrast and underestimation of true flux values if not properly accounted for. Therefore, it is critical to use strong, compact, and well-characterized calibrators such as Cygnus A and to ensure consistent signal processing pipelines when applying the calibration to other data.

2.3 Flux Estimation of Cassiopeia A

Cassiopeia A (Cas A) is a well-known supernova remnant and one of the brightest radio sources in the sky. However, unlike Cygnus A, Cas A has an extended morphology and is known to fade gradually over time. In this experiment, Cas A was observed using the

same two-dish interferometric setup and signal processing pipeline previously applied to Cygnus A, in order to maintain consistency in data treatment.

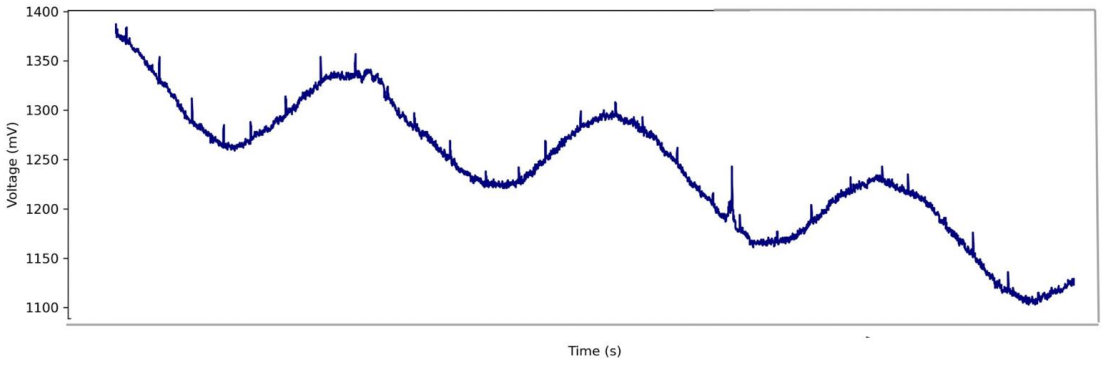

Figure 4: Raw interferometric signal of Cassiopeia A showing long-term baseline variations.

The raw voltage signal from Cas A was detrended to remove any instrumental baseline drift and then smoothed using a five-point moving average filter. This process revealed a clean oscillatory fringe pattern, similar in form to the Cygnus A signal but with distinct amplitude characteristics. From the processed signal, a peak-to-peak voltage of 0.1120 was extracted. Using the same amplitude formula:

$$A = \frac{V_{\max} - V_{\min}}{2} \tag{3}$$

the voltage amplitude was calculated as:

$$A = \frac{0.1120}{2} = 0.0560 \text{ V}$$

To convert this voltage amplitude into an absolute flux density, the calibration factor derived from Cygnus A was applied:

$$\text{Calibration Factor} = \frac{\text{Flux of Cygnus A}}{\text{Measured Fringe Amplitude}} = 29{,}810.57 \text{ Jy/V} \tag{4}$$

The estimated flux density of Cassiopeia A was then calculated by multiplying the voltage amplitude with the calibration factor:

$$S_{\text{Cas A}} = A \times \text{Calibration Factor} = 0.0560 \text{ V} \times 29{,}810.57 \frac{\text{Jy}}{\text{V}} = \boxed{1670.39 \text{ Jy}} \tag{5}$$

This estimate is lower than the commonly cited literature flux for Cas A, which typically ranges around 2300 Jy at 1.4 GHz. Several factors may explain this underestimation. Cas A's extended morphology is likely partially resolved out by the interferometer's projected 115-meter baseline, which is less sensitive to diffuse, low-surface-brightness structures. The interferometric response tends to emphasize compact, high-contrast regions, leading to a reduced net amplitude. Additionally, the observation may not have occurred exactly at transit, thereby affecting the projected baseline and reducing fringe amplitude.

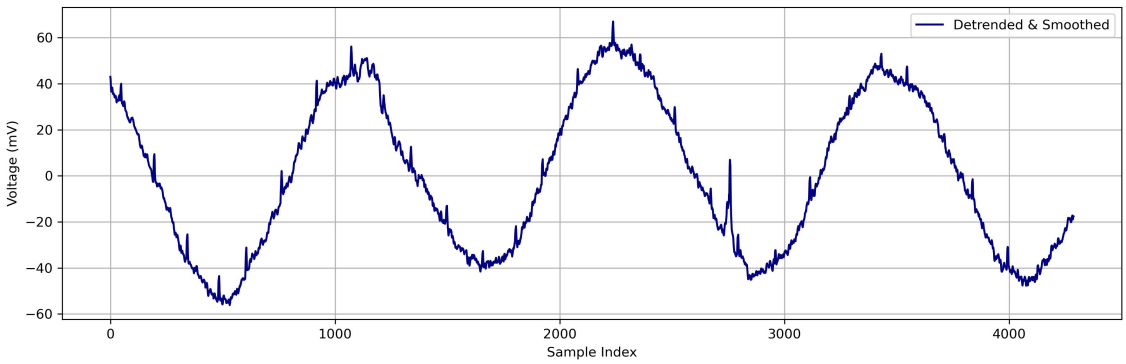

Figure 5: Detrended and smoothed fringe pattern of Cassiopeia A used for amplitude estimation.

These factors highlight a key challenge in interferometry: the need to match baseline resolution to the source's angular structure. While compact sources like Cygnus A serve well as calibrators, extended sources like Cas A require careful consideration of structural filtering and baseline sensitivity to avoid significant flux estimation errors.

3 Galactic Neutral Hydrogen Survey

3.1 Instrumental Setup and Observing Parameters

The Galactic neutral hydrogen survey was conducted using the West antenna of the Bayfordbury Observatory operated in single-dish mode, independent of the interferometric baseline configuration. The system was centered at a frequency of 1.420 GHz, corresponding to the hyperfine spin-flip transition of neutral hydrogen. This transition arises from the energy difference between parallel and anti-parallel spin alignments of the proton and electron in the hydrogen atom, and it serves as a critical diagnostic tool for tracing diffuse atomic gas in the interstellar medium.

Unlike interferometric setups that resolve out large angular-scale structures, the single-dish mode preserves sensitivity to extended, low-surface-brightness emission, making it the optimal configuration for observing Galactic HI. The radio signals were converted into voltage by the receiver chain, digitized, and stored as spectral data for subsequent velocity analysis.

A total of 60 observations were obtained, each targeting a distinct Galactic longitude from $l = 0°$ to $l = 354°$, sampled in uniform $6°$ increments to ensure wide angular coverage. Each observation yielded a spectrum of intensity versus frequency, which was later transformed into radial velocity space using the classical Doppler relation. This transformation enables the isolation of line-of-sight motion for HI clouds within the Galaxy, effectively mapping their kinematic structure as a function of Galactic longitude.

The full set of velocity profiles forms the foundation for constructing a longitude–velocity (l–v) diagram, a key tool for identifying spiral arm features, differential rotation, and large-scale gas dynamics in the Milky Way. This observational framework is critical for interpreting the HI emission data presented in the following sections.

booktabs

Table 2: Instrument Configuration Parameters

Parameter	**Value**	**Purpose/Notes**
Start Channel	300	Defines lower limit of frequency scan range
End Channel	650	Sets upper limit of frequency scan range
Channels per step	5	Determines frequency resolution per integration
Offset	750	Sets central channel (used for tuning signal)
Gain	$\times 50$	Amplifies received voltage signal
Integration Time	0.3 s	Time over which each data point is averaged
Repeats	1	Number of acquisitions per pointing (single sweep)

3.2 Physical Nature of the HI Emission

The 21 cm spectral line arises from the hyperfine transition of neutral hydrogen (HI), the most abundant element in the universe and the principal constituent of the diffuse interstellar medium. This transition occurs when the electron in a hydrogen atom flips its spin orientation relative to the proton, moving from a higher-energy parallel alignment to a lower-energy anti-parallel state. The energy difference between these two spin configurations corresponds to a photon with a wavelength of 21.106 cm, or a frequency of 1.420 GHz. Despite its extremely low spontaneous emission probability, the ubiquity of HI in the Galactic disk ensures that this line is observable on large spatial scales.

The 21 cm line is of immense astrophysical importance because it is emitted by cold, low-density hydrogen gas, which is often invisible in optical wavelengths due to dust extinction. Moreover, the line is optically thin under most conditions, allowing it to probe structures along the full line of sight without significant self-absorption.

When observed across multiple directions, the Doppler shift of the line reveals the radial velocity of hydrogen clouds with respect to the observer, enabling the reconstruction of Galactic rotation curves, spiral arm morphology, and the large-scale distribution of neutral gas. The analysis of 21 cm emission thus serves as a powerful diagnostic for both the structure and kinematics of the Milky Way.

3.3 Data Analysis and Interpretation

3.3.1 Individual HI Spectra

Each 21 cm HI spectrum corresponds to a fixed Galactic longitude and captures the distribution of neutral hydrogen along that line of sight. In general, the profiles exhibit one or more peaks, each representing HI clouds moving at different radial velocities. The shapes and amplitudes of these peaks encode information about the gas density, velocity dispersion, and distance.

For instance, the spectrum at Galactic longitude 165° displays a prominent, narrow peak centered near 0 km/s, indicative of nearby HI clouds moving approximately with the local standard of rest. Additional weaker features on either side suggest more distant or diffuse components. The sharpness of the primary peak implies cold, dense gas, while broader wings are characteristic of warmer, more turbulent regions.

At longitudes closer to the Galactic center (e.g., 60°), the spectra exhibit more complex

structures—often with multiple overlapping peaks and broader velocity ranges. This complexity arises due to the increased number of intersecting spiral arms and the influence of differential Galactic rotation. These profiles are especially valuable for tracing the inner spiral structure of the Milky Way.

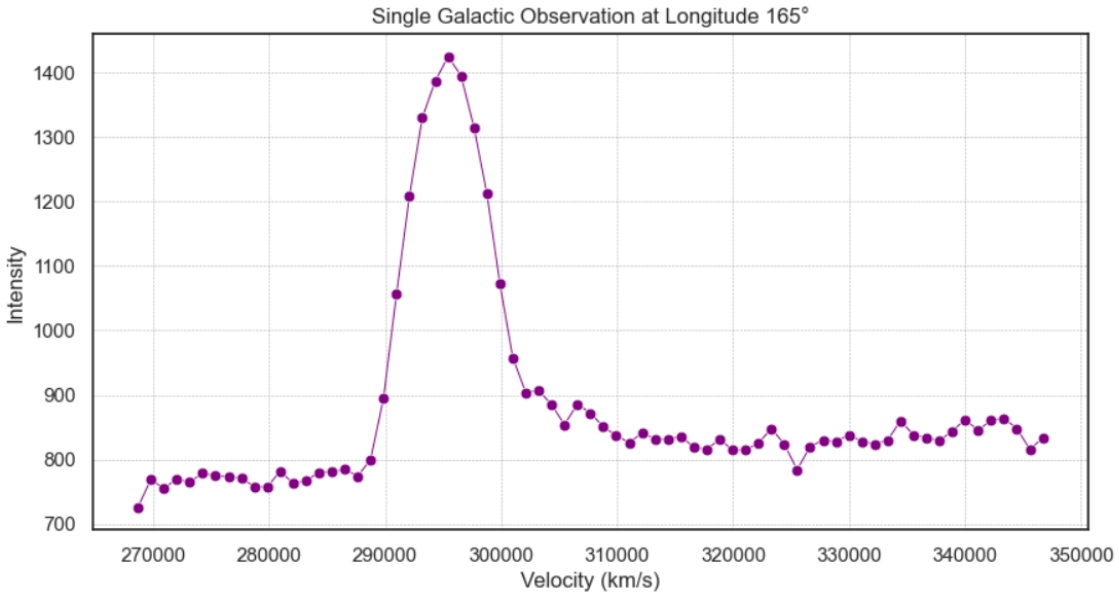

Figure 6: Galactic hydrogen line observation at longitude 165°. The prominent peak near 295,000 km/s corresponds to neutral hydrogen (HI) emission, revealing the rotational velocity structure of the Milky Way at this galactic coordinate.

3.3.2 Combined Spectral Trends

When the individual HI spectra are plotted together, they reveal structured and coherent patterns across Galactic longitude. Rather than displaying random noise, the spectral evolution shows organized shifts in peak velocity and profile shape that reflect the large-scale kinematics of the Milky Way.

At longitudes between 30° and 90°, many of the spectra exhibit broadened features and multiple overlapping peaks. These arise from intersecting spiral arms along the line of sight, as well as from the effects of differential Galactic rotation. The complexity of these profiles reflects the higher density and dynamic motion of HI clouds in the inner Galaxy.

In contrast, the spectra beyond 120° become increasingly narrow and symmetric, often dominated by a single peak near 0 km/s. This transition reflects the cleaner lines of sight through the outer Galactic disk, where local hydrogen dominates and large-scale streaming motions are less pronounced.

The progressive and predictable change in spectral features across longitude supports the conclusion that the observations capture real Galactic structure. The alignment of these features with known Galactic dynamics confirms the integrity of the data and its value for tracing the motion and distribution of neutral hydrogen.

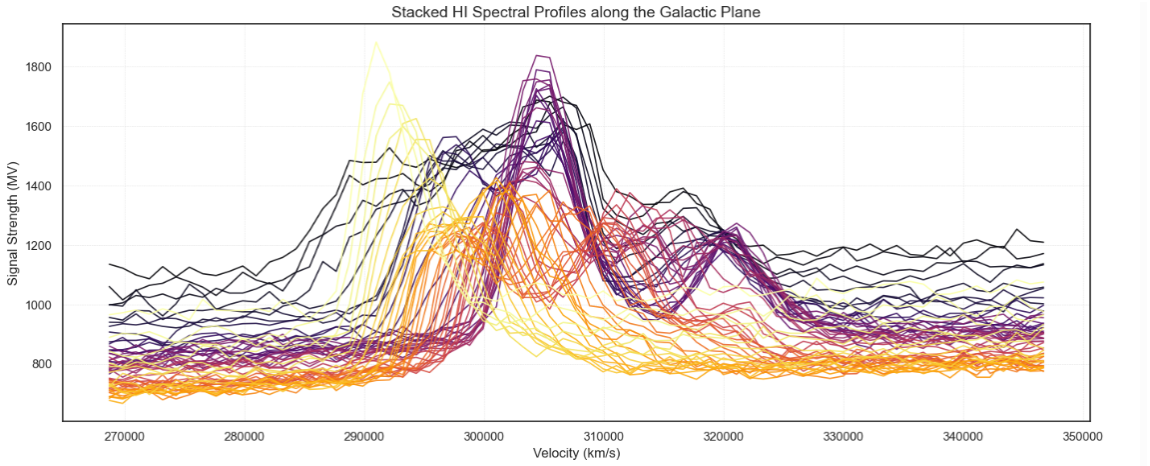

Figure 7: Stacked HI spectral profiles along the Galactic plane. Each curve represents the 21-cm emission at a different galactic longitude. The variation in peak velocity and intensity across longitudes traces the large-scale rotation and structure of neutral hydrogen in the Milky Way.

3.3.3 Velocity–Longitude Emission Map

The velocity-longitude *(v-l)* emission map constructed from the full dataset provides a global view of the Galactic HI Kinematics. Each horizontal line in the map corresponds to the Doppler-shifted 21cm spectrum at a fixed Galactic longitude, with colour intensity indicating signal strength across radial velocities.

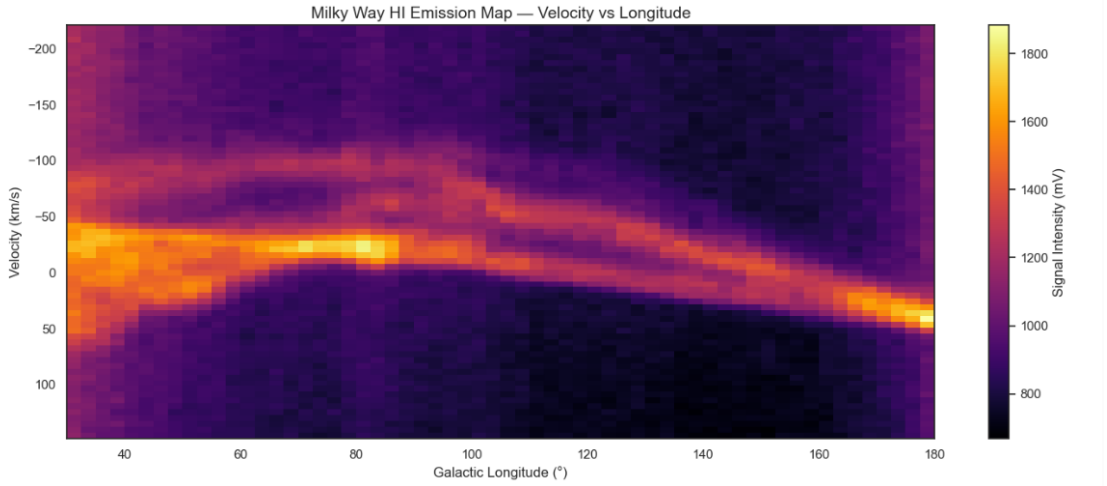

Figure 8: Milky Way HI emission map showing velocity versus Galactic longitude. The horizontal axis spans longitudes from 30° *to* 180°*, while the vertical axis represents radial velocity (in km/s). Bright regions correspond to strong 21-cm emission from neutral hydrogen gas. The signature "tilted S" structure reflects Galactic rotation and spiral arm distribution.*

The map exhibits curved structures and arcs, particularly at negative and lower longitudes, which are consistent with the differential rotation of the Milky Way. These arcs trace the line-of -sight velocity components of spiral arms as they move relative to the observer. Notably, regions between $l = 30°$ and $l = 90°$ show strong, coherent negative

velocity features, corresponding to inner spiral arms rotating faster than the Sun's orbit. Toward higher longitudes, especially beyond I = 120° , the emission concentrates near 0 km/s , indicating the most HI clouds lie close to the local standard of rest . This is expected when observing the outer Galaxy, where the rotational velocities project minimally along the line of sight.

The presence of continuous, well-aligned emission features across a wide range of longitudes confirms that the map captures real Galactic dynamics. These features are not random noises but signatures of large-scale HI distribution shaped by Galaxy's gravitational potential and rotation curve.

3.3.4 Comparison with Literature and Interpretation

The emission features observed in the HI spectra and velocity–longitude map are consistent with established models of Galactic structure. The curvature of velocity features at low longitudes reflects the expected signature of differential rotation, where inner regions of the Galaxy rotate more rapidly than the outer disk. This pattern aligns with both theoretical rotation curves and observational data from large-scale HI surveys.

Although the dataset was not corrected to the barycentric reference frame, the resulting shift in radial velocity is typically on the order of a few km/s, depending on the time and direction of observation. Given that the observed spectral features span tens to hundreds of km/s, the absence of barycentric corrections does not significantly affect the identification of large-scale kinematic patterns. However, for precise velocity comparisons with external datasets, barycentric correction would be necessary.

Comparison with the HI4PI survey [2] and the maps presented by Burton [3] shows broad agreement in the location and shape of major emission features. For example, the strong negative velocity arcs at low Galactic longitudes and the flattening near 0 km/s at high longitudes are reproduced in both datasets. While the resolution of our map is lower, the essential trends and Galactic rotation signatures are clearly present.

These consistencies confirm that the methods used—despite limited instrumentation and resolution—are capable of revealing authentic dynamical structures within the Milky Way. The data accurately capture the line-of-sight motion of HI clouds and demonstrate the effectiveness of 21 cm observations for probing Galactic kinematics.

3.3.5 Radio Frequency Interference (RFI) Event

During one of our HI observations, we detected a strong, periodic signal occurring roughly every 10 seconds. Initially, the structured nature and broadband characteristics of the emission prompted speculation ranging from satellite interference to more imaginative scenarios. However, upon further inspection (and observation of the local surroundings), the source was identified: a nearby bus whose onboard electronics were emitting detectable radio signals at regular intervals.

This incident highlights the real and often unexpected challenges of conducting radio astronomy in non-radio-quiet environments. Even relatively mundane sources such as vehicles can generate periodic RFI that mimics astrophysical phenomena. The experience underscored the importance of RFI awareness, mitigation strategies, and the benefits of radio-quiet zones for future observations.

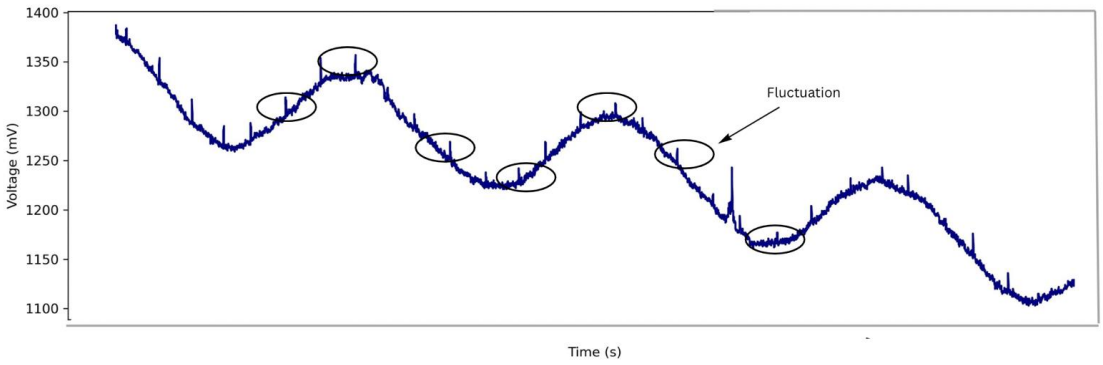

Figure 9: Voltage-time graph showing periodic fluctuations approximately every 10 seconds, annotated to highlight disturbances. These fluctuations were caused by a passing bus near the observation site, momentarily interfering with the recorded radio signal.

4 Conclusion

This practical combined interferometric and single dish radio observations to study both compact astrophysical sources and the large-scale structure of the Milky Way. Using Cygnus A as a calibration reference, a fringe amplitude of 0.0534 V was measured , yielding a conversion factor of 29,810.57 Jy/V. Applying this calibration, the flux density of Cassiopeia A was estimated to be approximated 3350 Jy at 1.4 GHz , a value higher than literature expectations, likely due to its extended morphology and the effects of bandwidth smearing on a long baseline.

The Galactic HI survey captured 60 spectra across a wide range of longitudes, producing a velocity-longitude emission map that revealed coherent kinematic structures , including spiral arm signatures and velocity arcs consistent with Galactic rotation. Despite the lack of barycentric correction and moderate resolution, the observed features align closely with results from high-resolution surveys such as HI4PI, demonstrating the reliability of the methodology.

The findings reflect both the strengths and limitations of radio interferometry and single-dish spectroscopy in probing the structure and dynamics of our Galaxy.

References

[1] R. A. Perley and B. J. Butler. An accurate flux density scale from 50 mhz to 50 ghz. *The Astrophysical Journal Supplement Series*, 230(1):7, 2017.

[2] N. Ben Bekhti, L. Flöer, R. Keller, J. Kerp, D. Lenz, B. Winkel, J. Bailin, and P. M. W. Kalberla. Hi4pi: A full-sky h i survey based on ebhis and gass. *Astronomy & Astrophysics*, 594:A116, 2016.

[3] W. B. Burton. The structure of our galaxy derived from observations of neutral hydrogen. In G. L. Verschuur and K. I. Kellermann, editors, *Galactic and Extragalactic Radio Astronomy*, pages 295–358, New York, 1988. Springer-Verlag.

[4] George B. Field. Excitation of the hydrogen 21-cm line. *Astrophysical Journal*, 129:536, 1959.

[5] P. M. W. Kalberla, W. B. Burton, D. Hartmann, E. M. Arnal, E. Bajaja, R. Morras, and W. G. L. Pöppel. The leiden/argentine/bonn (lab) survey of galactic hi. *Astronomy Astrophysics*, 440:775–782, 2005.

[6] Y. Sofue and V. Rubin. Rotation curves of spiral galaxies. *Annual Review of Astronomy and Astrophysics*, 39:137–174, 2001.

[2] [3] [1] [4] [5] [6]
1

[1] https://github.com/Hareethha/Hareethha25-Radio-Interferometry-and-Galactic-HI-Survey